

# Effects of ZrCuAl Bulk Metallic Glasses Poisson's Ratios on Spalling Process Induced by Laser Shock.

B. Jodar<sup>1,a)</sup>, D. Loison<sup>1,b)</sup>, Y. Yokoyama<sup>2</sup>, E. Lescoute<sup>3</sup>, C. Dereure<sup>1</sup>, M. Nivard<sup>1</sup>,  
H. Orain<sup>1</sup>, L. Berthe<sup>4</sup> and J.-C. Sangleboeuf<sup>1</sup>

<sup>1</sup>*Institute of Physics Rennes, UMR CNRS 6251, Rennes, France.*

<sup>2</sup>*Institute for Material Research, Tohoku University, Sendai, Japan.*

<sup>3</sup>*CEA/DAM/DIF, Arpajon, France*

<sup>4</sup>*PIMM, UMR CNRS 8006, Paris, France*

<sup>a)</sup>Corresponding author: benjamin.jodar@univ-rennes1.fr

<sup>b)</sup>didier.loison@univ-rennes1.fr

**Abstract.** To face High Velocity Impacts, the aerospace industry has a constant need for innovative materials that can be used as debris shielding components. Bulk Metallic Glasses (BMG) revealed interesting mechanical properties in case of static and quasi-static loading conditions: high elasticity, high toughness, low density and high fracture threshold. The department of Mechanics and Glass of the Institute of Physics Rennes conducted laser shock experiments (ELFIE facility) to study compositional effects on the behavior of a ternary ZrCuAl BMG under high strain rate, up to the fragmentation process. Ejecta velocities were measured by Photonic Doppler Velocimetry and debris morphologies were observed by shadowgraphy. Scanning Electron Microscopy observations revealed the influence of the composition on fracture surfaces morphologies. A dependency of spalling process has been correlated to Poisson's ratio (i.e. zirconium content).

## INTRODUCTION

For decades, it has been widely proven that metallic glasses possess very distinctive properties that contrast with other families of materials. On one hand, they exhibit macroscopic brittle fracture and shear localization at room temperature and under quasi-static loadings. At the microscopic scale on the other hand, evidences of plastic shear flows are usually observed on fracture surfaces with the appearance typical vein-patterns. Fracture in metallic glasses is also clearly unusual since some compositions are doted of high yield strength and toughness. To characterize their fracture behavior, extensive works have been focused on the correlation between elastic constants and toughness (or fracture toughness) [1], [2], [3], [4], [5]. As a result, ductility and brittleness but also atomic bonds are often discussed in term of Poisson's ratio: the higher this ratio is, the higher the ductility (plasticity) is. More precisely, Greer et al [6] suggested that within a given system (here a ternary one) a higher plasticity or toughness is always correlated with a higher  $\nu$ .

## EXPERIMENTAL SETUP

The ZrCuAl BMG ingots that were studied, were prepared by arc melting mixtures of high purity Zr (from a Zr crystal rod < 0.05 at. % oxygen), Cu and Al under an argon atmosphere. The full casting method is described in [7]. X-ray diffractometry was used to control that the cast ingot is amorphous. Initial properties summarized in Table 1 such as density and elastic moduli ( $E$  and  $\nu$ ) were measured respectively by Archimedes and ultrasonic method at room temperature. Four master ingots of ternaries  $Zr_xCu_{(90-x)}Al_{10}$  BMG ( $x = 45, 50, 55$  and  $60$ ) were cut and polished into slices of various thickness between 150 and 500  $\mu m$ . The experiments were performed at the ELFIE facility (UMR 7605, Ecole Polytechnique, France). Laser provides a 350  $fs$  duration high power pulse at 1.06  $\mu m$  -wavelength focused on the surface of the specimen (spot diameter of 1.7  $mm$ ). Samples are set in a secondary vacuum chamber

( $10^{-5}$  mbar is achieved) to avoid laser breakdown with air. The maximum provided energy is 11.4 J resulting in laser intensities up to  $1.38 \text{ PW.cm}^{-2}$ . Every shot was performed at quasi-identical energy ( $\sim 10.5 \text{ J} \pm 0.75$  corresponding to  $1.3 \text{ PW.cm}^{-2}$  intensity). In-situ diagnostics, such as Transverse Shadowgraphy [8] and Photonic Doppler Velocimetry (PDV) [9], [10] were used to follow ejecta trajectories and morphology, but also to measure spall velocities. The detailed description of the setup configuration is described elsewhere [11]. Post-mortem observations were performed on recovered fracture surfaces by a Scanning Electron Microscopy (SEM) on the ScanMat facility (UMS 2001, Rennes, France). To simplify reading in the following figures, compositions are depicted by four different colors: red, blue, yellow and green that correspond respectively to  $\text{Zr}_{45}\text{Cu}_{45}\text{Al}_{10}$ ,  $\text{Zr}_{50}\text{Cu}_{40}\text{Al}_{10}$ ,  $\text{Zr}_{55}\text{Cu}_{35}\text{Al}_{10}$  and  $\text{Zr}_{60}\text{Cu}_{30}\text{Al}_{10}$ .

**TABLE 1.** Initial properties of as-cast samples of ternary  $\text{Zr}_x\text{Cu}_{(90-x)}\text{Al}_{10}$  BMG ( $x = 45, 50, 55$  and  $60$ ).  $\rho$ ,  $E$ ,  $\nu$ ,  $T_g$  refer respectively to the initial density, Young's modulus, Poisson's ratio, and the temperature of vitreous transition

Composition	$\rho$ [ $\text{g.cm}^{-3}$ ]	$E$ [MPa]	$\nu$	$T_g$ [K]
$\text{Zr}_{45}\text{Cu}_{45}\text{Al}_{10}$	219	$97 \pm 1$	$0.354 \pm 0.002$	724 [12]
$\text{Zr}_{50}\text{Cu}_{40}\text{Al}_{10}$	225	$89 \pm 1$	$0.369 \pm 0.002$	706 [12]
$\text{Zr}_{55}\text{Cu}_{35}\text{Al}_{10}$	226	$87 \pm 1$	$0.370 \pm 0.002$	688 [12]
$\text{Zr}_{60}\text{Cu}_{30}\text{Al}_{10}$	223	$82 \pm 1$	$0.375 \pm 0.002$	671 [12]

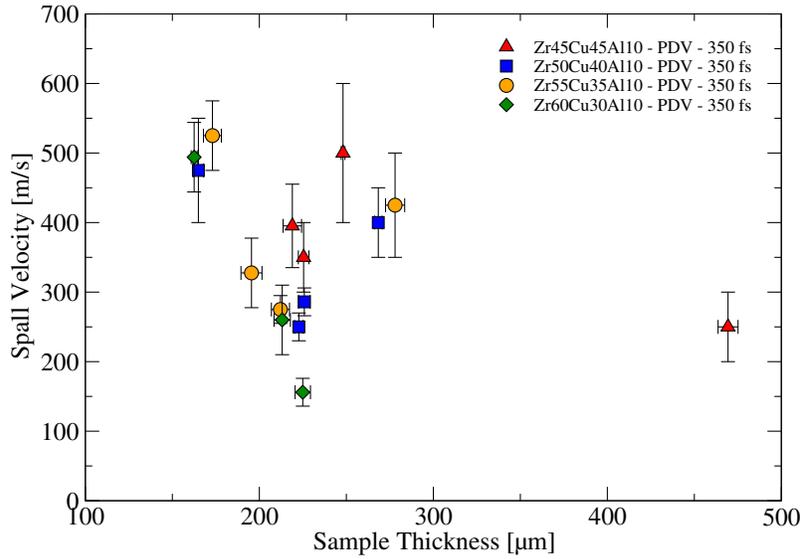


**FIGURE 1.** Spall velocity evolution versus sample thickness of  $\text{Zr}_x\text{Cu}_{(90-x)}\text{Al}_{10}$  samples ( $x = 45$  red triangle,  $x = 50$  blue square,  $x = 55$  yellow circle, and  $x = 60$  green diamond) subjected to  $1.3 \text{ PW.cm}^{-2}$  intensity laser shock.

## RESULTS

In Fig. 1 are displayed the terminal spall velocities measured by PDV versus sample thickness. According to shock-wave theory, spall velocity decreases with increasing sample thickness in between 150 and 270  $\mu\text{m}$  due to hydrodynamic damping [13], [14]. It appears for a fixed thickness that spall velocities are the highest for the Cu-richest composition ( $\text{Zr}_{45}\text{Cu}_{45}\text{Al}_{10}$ ) and the lowest for the Zr-richest specimens ( $\text{Zr}_{60}\text{Cu}_{30}\text{Al}_{10}$ ). However, at around 270  $\mu\text{m}$  one may distinguish a velocity jump for every composition except for the  $\text{Zr}_{60}\text{Cu}_{30}\text{Al}_{10}$  composition which did not spall. This jump is quite astonishing since BMGs do not apparently possess phase, unlike to crystalline materials. Somehow pressure level and/or sound wave velocity and/or dynamic tensile threshold are modified for samples thicker than 270  $\mu\text{m}$ . Furthermore, only the  $\text{Zr}_{45}\text{Cu}_{45}\text{Al}_{10}$  sample is subjected to spallation when sample thickness is around 460  $\mu\text{m}$ . For every shot, a single spall is ejected (Fig. 2) but these are less damaged in the case of high

zirconium rate specimens (Fig. 2 (c) and (d) in comparison with (a) and (b)). Finally, SEM magnifications of fracture surfaces are displayed in Fig. 3. Shots on  $Zr_{45}Cu_{45}Al_{10}$  and  $Zr_{50}Cu_{40}Al_{10}$  samples exhibit flat areas characteristic of brittle fracture. On the opposite, pictures ( $Zr_{55}Cu_{35}Al_{10}$ ) and ( $Zr_{60}Cu_{30}Al_{10}$ ) highlight a substantial amount of cavities as usually observed on fracture surfaces of ductile materials subjected to shockwave [15].

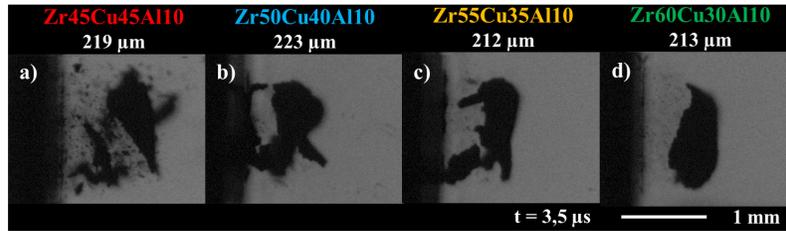


**FIGURE 2.** Transverse shadowgraphy of  $Zr_{45}Cu_{45}Al_{10}$ ,  $Zr_{50}Cu_{40}Al_{10}$ ,  $Zr_{55}Cu_{35}Al_{10}$ , and  $Zr_{60}Cu_{30}Al_{10}$  samples at  $3.5 \mu s$  after a  $1.3 PW.cm^{-2}$  intensity laser-shot. Every shot was in identical laser conditions (energy, duration, spot diameter and sample thickness).

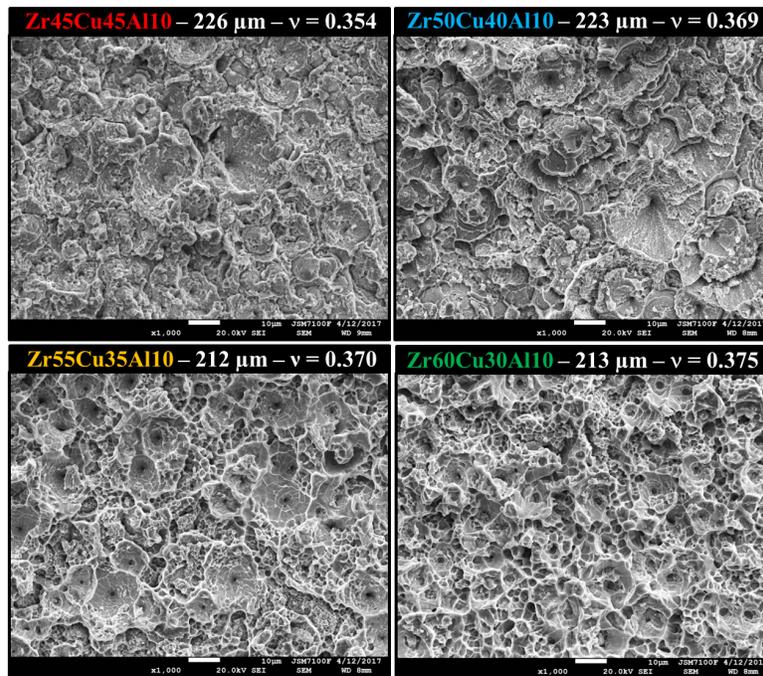


**FIGURE 3.** SEM magnification of spalled areas of  $Zr_{45}Cu_{45}Al_{10}$ ,  $Zr_{50}Cu_{40}Al_{10}$ ,  $Zr_{55}Cu_{35}Al_{10}$ , and  $Zr_{60}Cu_{30}Al_{10}$  samples recovered after  $1.3 PW.cm^{-2}$  laser-shock. Corresponding Poisson's ratios (related to zirconium content) are indicated.

## DISCUSSION

From these results, it seems that zirconium content plays a significant role on: terminal spall velocities and morphologies but also on fracture surfaces. Indeed, spall velocity decreases as Zr-rate increases. This can be attributed either to a more pronounced hydrodynamic damping or a higher dynamic tensile threshold. Time resolution of PDV did not allow to determine either the velocity when shockwaves break out at the free-surface nor the pull-back signal. Hence, it is currently not possible to discriminate the role of these two points on our results. Now, if one considers spall morphologies of shots on  $220 \mu m$  thick samples of each composition as depicted in Fig. 2, it appears that Zr-rate has also

an effect on the spall brittleness. This is also confirmed by fracture surfaces morphologies in Fig. 3. All these observations suggest that more energy is dissipated in Zr-rich samples. This composition dependency can be correlated with Poisson's ratio which, as shown in Table 1, increases with zirconium content. According to Lewandowski et al [2] and Greer et al [6],  $Zr_{60}Cu_{30}Al_{10}$  samples are supposed to exhibit the most ductile behavior and  $Zr_{45}Cu_{45}Al_{10}$  the least (possibly brittle). This is clearly in agreement with our results where an increasing Zr-content implies: lower spall velocity, less damaged i.e. more massive ejected spalls and finally more ductile fracture surfaces. To understand the fundamental reasons for this scaling to occur, one would have to look for the Short-Range- and Medium-Range-Order in the atomic bonding differences of these four compositions, but this is beyond the scope of this work. As for the velocity jump observed around  $270 \mu m$ , we are still unable to explain the phenomena responsible for it. Nonetheless, it has been widely reported that metallic glasses exhibit various rheological domains under high-temperatures and moderate strain rates ( $< 10^3 s^{-1}$ ) so that a deformation map regrouping decades of research has been established by Schuh et al [16]. It would be reasonable to consider these rheological effects to happen also under shock. Sadly, there is currently no data on plastic flow levels at dynamic strain rate ( $> 10^3 s^{-1}$ ), which paves the path for future works.

## CONCLUSION

To summarize, compositional effects of a ternary ZrCuAl BMG on spalling process was investigated by laser-shock. Velocity measurements, transverse observations of spall morphologies and fracture surfaces revealed a significant dependency of Poisson's ratio on the fracture behavior of this ternary system. Poisson's ratio increases with zirconium rate and Zr-rich compositions emphasize lower spall velocities, less fragmentation and a ductile fracture surface. As a result, during spallation more energy is dissipated in Zr-rich compositions. However, a peculiar jump velocity was observed for every composition for a thickness around  $270 \mu m$ . This particularity might be attributed to rheological effects usually observed in BMGs under quasi-static loadings.

## ACKNOWLEDGMENTS

The authors express their gratitude to all the LULI and SCANMAT staffs for technical support. The access to the LULI facility was provided through the Institute Laser Plasma (ILP, FR2707). This work was supported by DGA and ARED grants.

## REFERENCES

- [1] J. Schroers and W. L. Johnson, *Phys. Rev. Letters* **93**,255506 (2004).
- [2] J. J. Lewandowski, W. H. Wang, and A. L. Greer, *Phil. Mag. Letters* **85**:2, 77–87 (2005).
- [3] M. F. Ashby and A. L. Greer, *Scripta Materialia* **54**, 321–326 (2006).
- [4] S. J. Poon, A. Zhu, and G. J. Shiflet, *Appl. Phys. Letters* **92**, 261902 (2008).
- [5] Z. Q. Liu and F. Zhang, *J. Appl. Physics* **115**, 163505 (2014).
- [6] A. L. Greer, Y. Q. Cheng, and E. Ma, *Mat. Sci. Eng. R* **74**, 71–132 (2013).
- [7] Y. Yokoyama, A. Kobayashi, K. Fuhaura, and A. Inoue, *Mat. Transactions* **43**:3, 571–574 (2002).
- [8] E. Lescoute, T. D. Ressayguier, J.-M. Chevalier, M. Boustie, J.-P. Cuq-Lelandais, and L. Berthe, *Appl. Phys. Letters* **95**, 211905 (2009).
- [9] O. T. Strand, D. R. Goosman, C. Martinez, and T. L. Whitworth, *Rev. Sc. Instruments* **77**, 083108 (2006).
- [10] P. Mercier, J. Benier, A. Azzolina, J.-M. Lagrange, and D. Partouche, *J. Phys. IV* **134**, 805–812 (2006).
- [11] D. Loison, T. D. Ressayguier, A. Dragon, P. Mercier, J. Benier, G. Deloison, E. Lescoute, and A. Sollier, *J. Appl. Physics* **112**, 113520 (2012).
- [12] Y. Yokoyama, T. Ishikawa, J. T. Okada, Y. Watanabe, S. Nanao, and A. Inoue, *J. Non-Crys. Solids* **355**, 317–322 (2009).
- [13] M. Boustie and F. Cottet, *J. Appl. Physics* **69**, 7533–7536 (1991).
- [14] J.-P. Cuq-Lelandais, M. Boustie, L. Soulard, L. Berthe, T. D. Ressayguier, P. Combis, J. Bontaz-Carion, and E. Lescoute, *EPJ Web of Conferences* **10**, 00014 (2010).
- [15] T. Chen, Z. X. Jiang, H. Peng, H. L. He, L. L. Wang, and Y. G. Wang, *Strain* **51**, 190–197 (2015).
- [16] C. A. Schuh, T. C. Hufnagel, and U. Ramamurty, *Acta Materialia* **55**, 4067–4109 (2007).